Soil Dynamics and Earthquake Engineering 122 (2019) 79–93

Contents lists available at ScienceDirect

Soil Dynamics and Earthquake Engineering

journal homepage: www.elsevier.com/locate/soildyn

# Seismic soil classification of Italy based on surface geology and shear-wave velocity measurements

Giovanni Forte[a], Eugenio Chioccarelli[b,*], Melania De Falco[a], Pasquale Cito[c], Antonio Santo[a], Iunio Iervolino[c]

[a] Dipartimento d'Ingegneria Civile, Edile e Ambientale, Università degli Studi di Napoli Federico II, Via Claudio 21, 80125, Naples, Italy
[b] Università Telematica Pegaso, Piazza Trieste e Trento 48, 80132, Naples, Italy
[c] Dipartimento di Strutture per l'Ingegneria e l'Architettura, Università degli Studi di Napoli Federico II, Via Claudio 21, 80125, Naples, Italy

ARTICLE INFO

*Keywords:*
Probabilistic seismic hazard assessment
Regional seismic risk
Site classification
Soil classes
Seismic soil response

ABSTRACT

During an earthquake the seismic wave amplification related to local site conditions can have a significant impact on the ground motion. In order to account for these local effects some proxies for the soil characteristics exist; e.g., the average shear-wave velocity of the upper 30 m ($V_{S,30}$), or the equivalent shear-wave velocity from the ground to the depth of the seismic bedrock when this is less than 30 m ($V_{S,eq}$).

The aim of this paper is to provide maps of seismic shallow soil classification for Italy accounting for two sources of information: site-specific measurements and large-scale geological maps. The soil maps are obtained via a four-step procedure: (1) a database of available site-specific investigations is built, covering (unevenly) the whole national territory; (2) twenty geo-lithological complexes are identified from the available geological maps; (3) the investigations are grouped as a function of the geo-lithological complex and the distribution of measured $V_{S,30}$ and $V_{S,eq}$ are estimated; (4) medians and standard deviations of such distributions are assumed to be representative of the corresponding complexes. The statistics of investigations are used to derive the large-scale soil maps. To make the results of the study available, a stand-alone software has been developed. Despite not being adequate substitutes of site-specific studies such as microzonation and local site response analyses, the provided results can be useful for large-scale seismic risk studies.

## 1. Introduction

Seismic fault ruptures generate waves that propagate in all directions through the rigid bedrock for kilometres. Before reaching the ground surface, seismic waves go through the shallower materials covering the bedrock. It is known that this last part of propagation may have significant effects on a number of ground motion parameters (e.g., peak ground acceleration, spectral ordinates, etc.). Indeed, the so-called local site effects are deeply discussed in the literature (e.g., Ref. [1]) and must be taken into account for the estimation of seismic effects on structures. This is pointed out in the landmark papers by Dobry and Vucetic [2] and Seed et al. [3] and is systematically confirmed by the distribution of observed damages after significant earthquakes (e.g., Refs. [4–6]). In the hypothesis of a uniform layer of isotropic, linear elastic soil overlying rigid bedrock, the soil amplification of a harmonic horizontal motion of the bedrock is a function of (i) the thickness of the soil layer and (ii) the propagation velocity of shear-waves. In real cases, seismic wave propagation is more complicated and *site response analysis* is required to characterize the peculiar soil dynamics (e.g., Refs. [7,8]). However, for the cases in which such analyses cannot be performed, a simplified parameter to account for the site response, the average shear-wave velocity of the upper 30 m, $V_{S,30}$, was proposed at the end of the last century ([9,10]). $V_{S,30}$ is defined as per Equation (1) where $N$ is the number of homogeneous soil layers up to thirty meters depth whereas $h_i$ and $V_{S,i}$ are the thickness and the shear-wave velocity ($V_S$) in the soil layer $i$, respectively.

$$V_{S,30} = \frac{30}{\sum_{i=1}^{N} \frac{h_i}{V_{S,i}}} \tag{1}$$

The depth of 30 m was conventionally assumed as relevant (it is, typically, a depth that can be attained in one working day of boring). The value of $V_{S,30}$ has the advantage of being easily obtainable, at relatively low cost, by performing in-hole (*Down-Hole* or DH, *Cross-Hole* or CH), or surface (SASW, MASW, Microtremors) geophysical tests (e.g.,

* Corresponding author.
*E-mail addresses:* giovanni.forte@unina.it (G. Forte), eugenio.chioccarelli@unipegaso.it (E. Chioccarelli), melania.defalco@unina.it (M. De Falco), pasquale.cito@unina.it (P. Cito), santo@unina.it (A. Santo), iunio.iervolino@unina.it (I. Iervolino).

https://doi.org/10.1016/j.soildyn.2019.04.002
Received 11 October 2018; Received in revised form 1 March 2019; Accepted 1 April 2019

Ref. [11]). Furthermore, several scientific studies (e.g. Refs. [12–14]) provided strategies to infer $V_{S,30}$ values from the most common in-field tests, such as standard penetration test (SPT) or cone penetration test (CPT).

Today, $V_{S,30}$ is the main single-value parameter that summarizes seismic soil behaviour. The majority of the ground motion prediction equations (GMPEs) refer to $V_{S,30}$ either by (i) directly considering the $V_{S,30}$ value in the functional form (e.g., Refs. [15–18]); (ii) categorizing the soil behaviour (e.g., stiff or soft soil) depending on $V_{S,30}$ intervals and defining dummy variables associated to each soil category (e.g., Refs. [19,20]) or (iii) allowing both of these strategies (e.g., Refs. [21,22]). $V_{S,30}$ is also adopted by several seismic codes to identify the appropriate site-dependent design spectrum for structures; some examples are NEHRP Provisions [23] and the Eurocode 8, or EC8 [24].

On the other hand, several authors highlighted that knowledge of $V_{S,30}$ may not be enough to properly quantify the variation of seismic motion from bedrock to ground surface (see for example [25–28]). Indeed, it is known that the overall tendency of $V_S$ is to increase with depth; nevertheless, actual soil profiles may exhibit a shallow velocity inversion, due to the soil depositional variability along the profiles, which is reflected in peculiar characteristics of the seismic signal propagated through them. This case, in fact, cannot be detected if only the $V_{S,30}$ parameter is considered. Similarly, $V_{S,30}$ is not able to account for non-linear soil behaviour, for the actual depth of seismic bedrock, for deep soft deposits lying on much stiffer rock, for velocity profiles that do not exhibit a strong impedance contrast in the first meters or in basin-type geological settings. Thus, in the last years, scientific efforts have been made to develop and update classification criteria based on $V_{S,30}$ together with other relevant parameters, such as the bedrock depth (e.g., Ref. [29]), or site period/frequency (e.g., Ref. [30]).

In accordance with this trend, the recent Italian building code, or ItBC2018 [31], tries to overcome some of the $V_{S,30}$ limitations (those related to bedrock depth), by referring to the so-called $V_{S,eq}$, which derives from a slight modification of the $V_{S,30}$ parameter. This is defined in Equation (2), in which $H$ is the depth of the bedrock if it is less than 30 m. When the bedrock is deeper, $H$ is equal to 30 (and $V_{S,eq}$ degenerates into $V_{S,30}$).

$$V_{S,eq} = \frac{H}{\sum_{i=1}^{N} \frac{h_i}{V_{S,i}}} \tag{2}$$

It should be noted that, although $V_{S,30}$ or $V_{S,eq}$ can be useful for a preliminary soil site classification, they cannot be considered as sufficient information for structural seismic risk assessment at a specific site. In this case, a number of additional parameters, such as the soil resonance frequency or the whole shear-waves profile to the bedrock would be required. On the other hand, in the case of a large area of interest (i.e., large-scale/regional seismic risk analyses), because more refined soil information is often impossible to acquire, $V_{S,30}$ (or $V_{S,eq}$) values are commonly considered as viable parameters. Moreover, in these cases, since actual measurements are usually available at a limited number of sites, strategies to extend the single-site evaluations to a broader area are often required. Several approaches have been proposed in both technical and scientific literature (see for instance Refs. [32,33]) based on geological, geomorphological or geotechnical units [34–39]. Thompson et al. [40] proposed a $V_{S,30}$ map for the California using a hybrid geostatistical approach able to account for geology, topography, and site-specific shear-wave velocity measurements. Although there is extensive literature on the topic, the most widespread method, due to its user-friendliness, is the United States Geological Survey (USGS) approach developed in Ref. [41]. The method is based on the use of a correlation between topographic slope and $V_{S,30}$; according to that method, steep slopes generally reflect rock formations, nearly-flat areas indicate soft soils and intermediate slopes correspond to stiff soils (the accuracy of results often depends on the resolution of the digital elevation model). Lemoine et al. and Forte et al. [42,43] compared the $V_{S,30}$ map predicted by USGS method for Mediterranean Europe and a case study in Italy with a fair collection of $V_S$ measurements. Both studies found that the USGS approach tends to overestimate the actual $V_{S,30}$ measurements.

In Italy, site classifications on a national scale have been made by the Italian *Istituto Nazionale di Geofisica e Vulcanologia* (INGV), which is responsible for providing the seismic hazard map for structural design in Italy. More specifically, Luzi and Meroni [44] proposed a national 1:500.000 map for site classification, based on a broad geological criterion considering lithology and age, and related to three ground types. Later, Michelini et al. [45] upgraded this map by classifying the geological units derived from the 1:100.000 geology map of Italy into five ground categories (from A to E). They correlated these categories to those specified by EC8 (see the next section), being characterized by the following reference $V_{S,30}$ values: (A) 1000 m/s; (B) 600 m/s; (C) 300 m/s; (D) 150 m/s; (E) 250 m/s, with soil thickness $<$ 20 m. The most recent map was provided by Di Capua et al. [46] based on 1:100.000 geological maps. It represents an attempt to merge geological formations in lithoseismic classes following their lithological description, in order to identify areas characterized by a homogeneous seismic response.

In the remainder of this paper, a four-step procedure for correlating the surface geological maps with site-specific investigations is presented. Then, referring to the Italian case, each step is quantitatively described. An intermediate result of the procedure is the assessment of medians and standard deviations of $V_{S,30}$ and $V_{S,eq}$ parameters for all the Italian sites. The final result is the soil classification, according to EC8 and ItBC2018, of the country. All results are provided by means of a software (available at http://wpage.unina.it/iuniervo/SSC-Italy.zip) that can be a useful tool for large scale seismic studies or post-earthquake shakemap generation (e.g., Refs. [47,48]). Finally, an illustrative application is carried out to quantify the effect of soil classification in the case of probabilistic seismic hazard analysis at a national scale.

## 2. Methodology

From 2008 until the beginning of 2018, the Ref. [49] was the national seismic code for structural design and assessment. Criteria for soil classification were in good accordance with the current version of EC8. The latter associates a soil class on the basis of $V_{S,30}$ assessment or, alternatively, on the values of SPT blow-count or the undrained shear strength of soil. The description of each soil class together with the $V_{S,30}$ intervals are reported in Table 1 for the sake of completeness. The $V_{S,30}$ parameter could be computed from the $V_S$ profiles that are characterized by a gradual increase of mechanical properties with depth. In the table, four main soil categories (from A to D) are identified for decreasing $V_{S,30}$. Then, three other classes (E, S1, S2) can be defined considering additional information.

In the new version of the Italian building code, ItBC2018, some differences in the criteria for soil site classification have been introduced. Site classification now refers to $V_{S,eq}$, the number of soil classes has been reduced to five and the definition of class E has been changed as reported in Table 2.

This paper provides statistics of $V_{S,30}$ and $V_{S,eq}$ values for the Italian sites that are used to derive a seismic soil classification on a national scale according to both EC8 and ItBC2018. Here the general procedure adopted in the study is summarized. The approach aims to account for two types of information that are (i) the site-specific investigations and $V_S$ measurements, and (ii) the existing geological maps that identify geographic area, or polygons, with homogeneous features. The procedure is summarized in four steps.

1. The first effort was the search and collection of the available data about investigations performed for any site of Italy. Retrieved information was analysed by the authors in order to obtain a dataset of geographical locations and soil classes. All data were stored in a geographical information system (GIS) database and, for each

**Table 1**
Ground type/Soil classification according to EC8.

| Ground type/Soil class | Description of stratigraphic profile | $V_{S,30}$ [m/s] |
|---|---|---|
| A | Rock or other rock-like geological formation, including at most 5 m of weaker material at the surface. | > 800 |
| B | Deposits of very dense sand, gravel, or very stiff clay, at least several tens of meters in thickness, characterized by a gradual increase of mechanical properties with depth. | 800–360 |
| C | Deep deposits of dense or medium-dense sand, gravel or stiff clay with thickness from several tens to many hundreds of meters. | 360–180 |
| D | Deposits of loose-to-medium cohesionless soil (with or without some soft cohesive layers), or of predominantly soft-to-firm cohesive soil. | < 180 |
| E | A soil profile consisting of a surface alluvium layer with Vs values of type C or D and thickness varying between about 5 m and 20 m, underlain by stiffer material with Vs > 800 m/s. | – |
| S1 | Deposits consisting, or containing a layer at least 10 m thick, of soft clays/silts with a high plasticity index (PI > 40) and high-water content. | < 100(indicative) |
| S2 | Deposits of liquefiable soils, of sensitive clays, or any other soil profile not included in types A – E or S1. | – |

investigation, the values of $V_{S,30}$ and $V_{S,eq}$ were calculated.
2. Starting from the original geological formations as classified by *Istituto Superiore per la Protezione e la Ricerca Ambientale* (ISPRA), a simplified geo-lithological classification was set up. The new classification accounts for similar lithology, geomorphologic setting, genetic processes (*facies*), age and seismic behaviour of the original categories. The geo-lithological classification polygons were digitized and implemented in the GIS database.
3. Data from step one and step two were combined: values of $V_{S,30}$ and $V_{S,eq}$ were grouped as function of the geo-lithological class in which they were measured and the statistics were computed for each class.
4. Finally, $V_S$ measurements were associated to each geo-lithological class, together with the first, second (median value) and third quartiles of the considered distributions. This allowed to provide $V_{S,30}$ and $V_{S,eq}$ median values and standard deviations for each geo-lithological complex. Additionally, as described in Section 6, combining the $V_S$ measurements with the other available information, each investigated site was classified according to soil classes proposed by EC8 and ItBC2018. This allowed to identify a more probable soil class for each geo-lithological complex which has been assumed as representative of the complex.

It should be noted that two new contributions can be identified in the procedure. First, this is, to authors' knowledge, the first attempt to collect the available measurements of soil shear-wave velocities on a national scale in Italy, combined with geo-lithological characteristics. This requires a significant effort in the search and homogenization of information and allows continuous enrichment of the database with new available investigations. Second, the identification of geo-lithological complexes and the association of $V_S$ statistics, as well as soil classes, to each complex have not been proposed before for Italy. Nevertheless, similar procedures were described in Refs. [37,43], which developed the maps for single Italian regions (Campania and Molise, respectively), using a smaller sample of $V_S$ measurements.

## 3. Available data (step one)

The authors collected data from a wide range of sources resulting in a strongly uneven distribution in both quantity and quality of the information. This is mainly because only some Italian administrative regions operate geological services that collect and distribute data; consequently there are no common standards about the data and format. More specifically, data used in this paper were retrieved from the following sources (see the Data Sources section for further details): available scientific and technical reports for the seismic characterization of the strong-motion stations of the Italian Accelerometric Archive (ITACA); reports from microzonation projects for the Abruzzo, Molise and Basilicata regions; regional databases of the seismic service of Emilia Romagna; Civil Protection studies for Sicilia and Trentino Alto-Adige regions; local site effects valuation Project for Toscana (VEL); local civil engineering practitioners; scientific reports; civil engineering projects and unpublished technical reports.

The collected data are considered reliable if the location is clearly defined and $V_S$ is measured through standard geophysical tests. This implies, for example, that $V_{S,30}$ values inferred through the most common or recent empirical correlations with penetration resistance (e.g., Refs. [12,14,30]) were excluded. Moreover, in some cases, available data are characterized by shear-wave velocity profiles that do not reach 30 m; these data were not used to compute $V_{S,30}$ even if several methods allow to infer it from shallow velocity profiles (e.g., Refs. [50–52]). These same data were adopted only to compute $V_{S,eq}$ when the depth of the bedrock is known. Apart from shear-wave velocity measurements, a number of sites have other relevant information as geological description of the study area, stratigraphic logs, and results of laboratory and field geotechnical tests.

The available in situ tests were uploaded as a database (DB) in a GIS environment. The DB consists of an identifier code for the different regions of Italy, UTM geodetic coordinates, type of investigation, data source, the shear-wave velocity at each depth (when available), that is $V_{S,z}$, and $V_{S,30}$ or $V_{S,eq}$ measurements. A detailed description of the

**Table 2**
Ground type/Soil classification according to ItBC2018.

| Ground type/Soil class | Description of stratigraphic profile | $V_{S,eq}$ [m/s] |
|---|---|---|
| A | Rock or other rock-like geological formation, including at most 3 m of weaker material at the surface. | > 800 |
| B | Deposits of very dense sand, gravel, or very stiff clay, at least several tens of meters in thickness, characterized by a gradual increase of mechanical properties with depth. | 800–360 |
| C | Deep deposits of dense or medium-dense sand, gravel or stiff clay with thickness higher than 30 m and characterized by a gradual increase of mechanical properties with depth. | 360–180 |
| D | Deposits of loose-to-medium cohesion soil with thickness higher than 30 m and characterized by a gradual increase of mechanical properties with depth. | 180–100 |
| E | Soils with characteristics and equivalent shear velocity analogous to those defined for classes C and D but with a deposits thickness not higher than 30 m. | – |

**Table 3**
Subset of data adopted for $V_{S,30}$.

| Investigation type | Seismic bedrock deeper than 30 m | Seismic bedrock less deep than 30 m | Only $V_{S,30}$ available | Total number of data |
|---|---|---|---|---|
| In-Hole tests | 607 | 903 | 60 | 1570 |
| Surface Geophysical Tests | 82 | 101 | 136 | 319 |
| Microtremors | 126 | 574 | 1237 | 1937 |
| **Total number of data** | 815 | 1578 | 1433 | 3826 |

database is reported in the following but, before proceeding any further, it is important to recall that the assessment of $V_{S,30}$ and $V_{S,eq}$ requires slightly different information, hence data were differently selected depending on the considered parameter.

The complete database features 3842 $V_S$ measurements. In sixteen cases, the $V_{S,z}$ profiles are extended to the bedrock depth, which is shorter than 30 m; thus, they cannot be used for the $V_{S,30}$ assessment. Therefore, two subsets of data of 3826 and 3842 measurements are used for $V_{S,30}$ and $V_{S,eq}$, respectively. As pertaining to $V_{S,30}$, Table 3 describes the DB in detail; the measurements come from different types of investigations: 1570 In-Hole Tests (DH, CH, SCPT), 319 Surface Geophysical Tests (MASW, SASW, seismic refraction surveys) and 1937 Microtremors (ESAC, Re.Mi., HVSR, Passive Array, FTAN) designed to measure shear-wave velocity profiles (ASTM D7400-08 [53]). For each type of investigation, the table shows the available information. For 1433 sites, only the $V_{S,30}$ value is available, whereas for 2393 sites the $V_{S,z}$ profile to 30 m depth is available; among these, for 815 sites, the seismic bedrock is less than 30 m deep while in the remaining 1578 it is deeper than 30 m.

The location of the collected data in terms of type of investigation is reported in Fig. 1. The figure shows that the overall data distribution clearly follows the Apennine mountain chain, where there is the largest seismic hazard [54], or identifies the areas affected by the most recent earthquakes (the magnitude, or M, equal to 6, Umbria-Marche earthquake, 1997; the M5.7 Molise earthquake, 2002; the M6.3 L'Aquila earthquake, 2009; the M6 Emilia sequence, 2012), where post-event studies provided a relevant number of investigations. It should also be noted that Microtremors provide a less accurate estimation of shear-wave velocity with respect to In-Hole Tests and Surface Geophysical Tests. Although Microtremors provide the highest percentage of data (about 45%), these kinds of test were concentrated in two regions: Emilia Romagna and Trentino Alto Adige. On the other hand, In-Hole Tests, which provide the most accurate information, are distributed over a large area covering the whole Apennine chain.

The preliminary screening of data provides slightly different results when the $V_{S,eq}$ is considered. In this case, investigations in which $V_{S,z}$ profiles reach the seismic bedrock can be used even if they do not reach the depth of 30 m (Table 4). Thus, a total of 3842 investigations are considered eligible for $V_{S,eq}$ identification. Among them, 2409 are those in which the entire $V_{S,z}$ profile to the bedrock is available (seismic bedrock is deeper than 30 m in 1578 sites whereas is less than 30 m deep in 831); for the remaining 1433 sites only the $V_{S,30}$ is available. In these cases, to avoid rejecting a large amount of data, it is assumed that the seismic bedrock is deeper than 30 m and consequently $V_{S,30}$ is equal to $V_{S,eq}$.

A preliminary classification is performed as a function of velocity intervals for both considered parameters. Considered intervals are those used by EC8 and ItBC2018 for soil class identification, that is, > 800 m/s, 800-360 m/s, 360-180 m/s and < 180 m/s. Classification results are reported in Fig. 2. According to the figure, most of the sites (51%) are in the 800-360 m/s interval of $V_{S,30}$, while the 38% are within 360–180 m/s. Fewer sites (5%) have $V_{S,30}$ higher than 800 m/s and 6% of sites are lower than 180 m/s. Similar are the results in terms of $V_{S,eq}$: 3% of sites are higher than 800 m/s, the majority (47%) are within 800–360 m/s, 44% are within 360–180 m/s and 6% are lower than 180 m/s. Site class A represents the seismic bedrock and is characterized by fewer investigations with respect to the others. This is due to the common practice of not performing geophysical investigations on rock outcrops (usually in mountainous settings). On the other hand, more efforts are usually addressed to the characterization of areas of towns or engineering works that, in Italy, mainly correspond to B and C soil classes.

## 4. Geo-lithological map (step two)

ISPRA is currently building the geological map of Italy at a 1:50.000 scale. It will cover the national territory with a total of 652 sheets but only 254 of them are available so far. Two hundred seventy-seven geological maps covering Italian territory produced by ISPRA at the 1:100.000 scale [55] are adopted for this study. They were completed in 1976 from field surveys performed on a 1:25.000 scale. Each geologic formation is characterized by lithological characteristics and age. However, similarly to other geological classifications on a national scale (see for example [56], for the case of Greece), it is easy to identify a lack of consistency at the boundaries of each sheet in which the territory is divided. This is due to the different interpretations and classifications made by geologists who carried out the survey in different years and adopting different classification criteria. In order to combine these national geological maps with the data described in the previous section, a simplified classification harmonizing the original categories was set up, involving expert judgement. With this aim, broader categories were introduced as function of similar lithology and geomorphologic setting, genetic processes (*facies*), age, and seismic behaviour. To give an example, all the original geological formations described as “gravel and sand coming from river and alluvial environment” were grouped, because these types of soil have, in general, very similar lithological features independently of the geographic location. Other examples are some geologic bedrocks such as “limestones” or “crystalline rocks".

In fact, a relevant distinction was based on the identification of geo-lithological complexes as *geologic bedrock* (Paleozoic to Pleistocene) versus those representative of *cover deposits* (Quaternary). Geologic bedrock formations were mainly grouped from a lithological and age point of view (note that geologic bedrock category is not directly related to defined values of $V_S$), while cover deposits were distinguished by depositional environment, also accounting for soil grain categories, as it is a general understanding that $V_S$ values increase passing from fine-grained soils to coarser ones. The followed approach permitted to summarize the Italian geological setting in eighteen geo-lithological complexes. Furthermore, an effort to better characterize some local Italian geological features can be found in the distinction in two different sub-complexes for Igneous metamorphic bedrock (IMB) and Lava bedrock (LB). Indeed, some Italian geographic areas experienced a different tectonic history, which strongly modified the fracturing states and resulted in the IMB1 and IMB2 sub-complexes. Meanwhile, LB1 and LB2 are characterized by a different magmatic composition, which strongly controlled the eruptive style and the consequent deposits [57]. These issues could affect the soil properties and the geo-lithological complexes considered hereafter are twenty. Each of them is described in Table 5, while the map representing the twenty identified complexes is reported in Fig. 3.

The identified complexes account for the overall geological formations existing in Italy; however, an analogous classification could be adopted in other countries, as all geological materials and environments

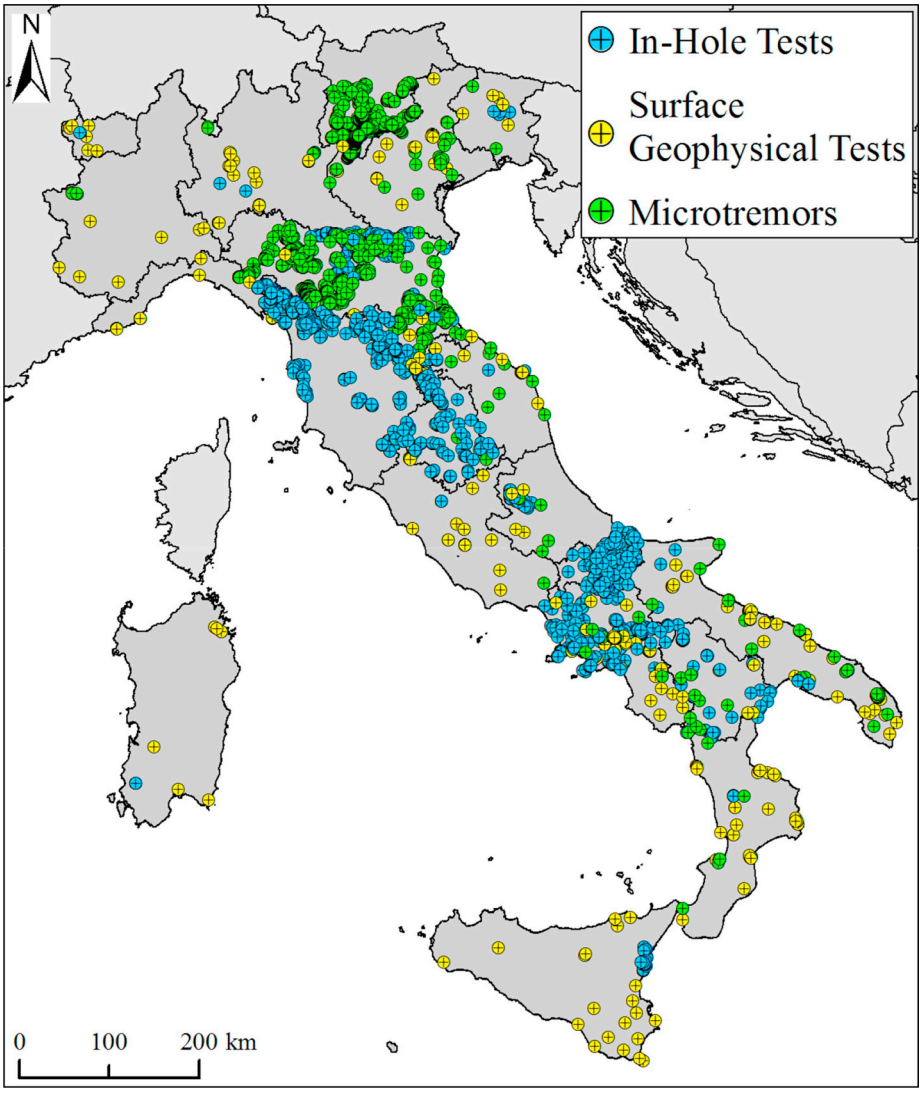


**Fig. 1.** Distribution and type of collected data.

identified in this classification can also be found worldwide.

## 5. Statistics of Vs values per geo-lithological complex (step three)

The $V_{S,30}$ and $V_{S,eq}$ measurements are grouped into the twenty geo-lithological complexes shown in Table 5. The statistics of $V_{S,30}$ data associated to each complex are computed and represented through the box-plots of Fig. 4 (numerical values of mean, median and standard deviations of data are reported in Appendix). In the same figure, the number of data for each geo-lithological complex are also shown (data in IMB1 are few and first and second quartiles cannot be graphically distinguished).

The first, second (median value), and third quartiles are reported together with the minimum and maximum values of the empirical distribution. Outliers are defined as the values that lie below the first quartile minus 1.5 times the interquartile range (IQR) or above the third quartile plus 1.5 times the IQR (e.g., Ref. [58]).

For the geologic bedrock formations, Fig. 4 shows that the distinction between the two sub-complex IMB1 and IMB2 resulted in differences of soil characteristics: median $V_{S,30}$ values are 805 m/s and 536 m/s, respectively. On the other hand, median values associated to LB1 and LB2 are almost equal (some differences between LB1 and LB2 appear when $V_{S,eq}$ is of concern, as shown in Fig. 5). All the other geologic bedrock complexes resulted in median $V_{S,30}$ between 360 and 800 m/s, with the exception of CB and SB, which have median value equal to 847 and 326 m/s, respectively. For Quaternary deposits, Fig. 4 shows that they are characterized by shear-waves velocity clearly decreasing as function of the grain-sizes, sorting and textures. Coarse

**Table 4**
Subset of data adopted for $V_{S,eq}$.

| Investigation type | Seismic bedrock deeper than 30 m | Seismic bedrock less deep than 30 m | Only $V_{S,30}$ available | Total number of data |
|---|---|---|---|---|
| In-Hole tests | 622 | 903 | 60 | 1585 |
| Surface Geophysical Tests | 83 | 101 | 136 | 320 |
| Microtremors | 126 | 574 | 1237 | 1937 |
| **Total number of data** | 831 | 1578 | 1433 | 3842 |

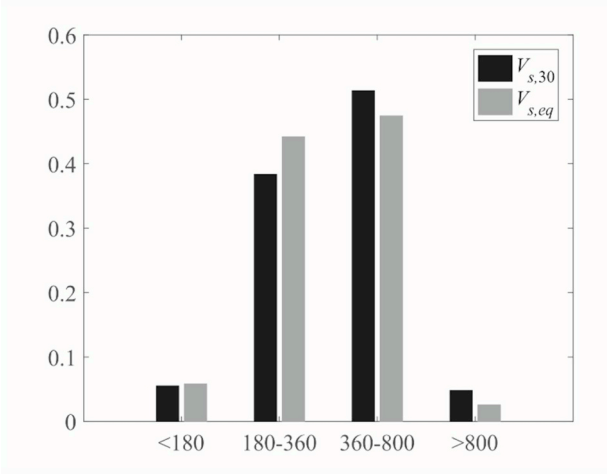


**Fig. 2.** Distribution of data with respect to $V_{S,30}$ and $V_{S,eq}$ .

gravel-grained and massive deposits, such as tv, mr, db and tcg, resulted in median $V_{S,30}$ between 360 and 800 m/s, finer deposits made of gravels and sands resulted within 180 and 360 m/s (gs, sd), while $V_{S,30}$ lower than 180 m/s was attributed to silts, clays and peats grouped in the csp complex. Finally, the distinction between ignimbrites (tfs) and pyroclastic soils (pyr), with the former being more lithic and the latter loose, resulted in two different intervals of $V_{S,30}$: between 360 and 800 m/s and 180 and 360 m/s, respectively.

An analogous classification is performed with respect to $V_{S,eq}$, as reported in Fig. 5. Results are in good accordance with those shown in the previous figure. The only differences are: (i) LB2 does not belong to the 360–800 m/s interval, having median value of 315 m/s; (ii) IMB2 has median value lower than 800 m/s and equal to 476 m/s. The latter are due to the definition of $V_{S,eq}$, which does not take in account the increase of stiffness provided by the seismic bedrock contribution.

## 6. Seismic soil classification of Italian sites (step four)

In the framework of this study, median and standard deviation values of $V_{S,30}$ and $V_{S,eq}$ of each geo-lithological complex are associated to all locations within a complex. This allows providing a soil characterization for the whole national territory that can be used in the case of large-scale seismic hazard/risk analysis.

Fig. 6 shows the maps of (a) $V_{S,30}$ and (b) $V_{S,eq}$ distribution for Italy coming from the median values identified from the box-plots of Figs. 4 and 5, respectively. The two maps display a similar shear-waves velocity distribution, with some differences for the values higher than 800 m/s, which are more present in Fig. 6a and the 180–360 m/s range, which in Fig. 6b replaces some sites identified in the range 360–800 m/s in Fig. 6a.

Fig. 6c reports the corresponding $V_{S,30}$ map of [45] for comparison. It shows a widespread distribution of sites characterized by values higher than 800 m/s, with fewer areas in the range 360–800 m/s. The sites having 180–360 m/s values are mainly concentrated in the North, while values less than 180 m/s are poorly represented.

Recall (Tables 1 and 2) that both EC8 and ItBC2018 classifications account for some soil classes that are not defined exclusively on the basis of $V_S$ measurements: these are class E, S1 and S2 for EC8 and class E for ItBC2018. Hence, some additional analyses of data are required to extend soil classification to code-conforming classes. More specifically, after having grouped data per geo-lithological complex, each site is classified in accordance with EC8 and ItBC2018. Thus, the frequency of soil class occurrence for each complex is computed and the most frequent (modal) soil class is assumed as the representative class of the whole complex.

According to this procedure, Fig. 7 shows the soil class frequencies in accordance with EC8 classification. In most cases, one soil class is predominant with respect to the others, but for CB and CtB the frequencies of A and B class occurrences are comparable as well as the frequencies of B and C classes for tcg and the frequencies of C and D classes for csp.

Comparing Figs. 4 and 7, it can be seen that site classification of the latter is in perfect accordance with the median $V_{S,30}$ values shown in the former. This is partially described by the fact that the number of investigations that assigned class E (the soil class not defined only on $V_{S,30}$ parameter) is negligible.

Soil class frequencies in accordance with ItBC2018 classification are reported in Fig. 8. For each complex, soil class attribution is the same as for EC8, except for LB2 and CB. Both these complexes display a significant presence of E site-class. Thus, an attempt to distinguish different local settings within the same complex is carried out. Topographic slope was assumed as a proxy for the identification of sub-areas.

**Table 5**
Geo-lithological complexes.

| Name of the Complex | ID | Description | Geologic Age |
|---|---|---|---|
| **Cover deposits** | | | |
| Pyroclastic soil | **pyr** | Successions of ashes, pumices and scoriae | Pleistocene-Holocene |
| Tuff and scoriae | **tfs** | Tuffs and ignimbrites | Oligocene - Pleistocene |
| Clay silt and peat | **csp** | Clays, silts, peat from palustrine environment | Pleistocene-Holocene |
| Sand | **sd** | Sands and gravels from dunes and beaches | Pleistocene-Holocene |
| Gravel and sand | **gs** | Conglomerates, gravels and sands from alluvial deposits. | Pleistocene-Holocene |
| Terraced conglomerate | **tcg** | Conglomerates, sands and shale from terraced successions. | Pleistocene |
| Shallow debris | **db** | Infill, alluvial fan, debris, colluvium, breccia, debris talus and sandy-silt talus on igneous and metamorphic bedrock. | Pleistocene-Holocene |
| Moraine | **mr** | Moraines deposits and large landslide bodies | Pleistocene - Holocene |
| Travertine | **tv** | Travertines and soft limestones | Pleistocene-Holocene |
| **Geologic Bedrock** | | | |
| Lava | **LB1** | Porphyries and lava | Paleozoic - Holocene |
| | **LB2** | Lava (Sardinia and Sicily) | Cenozoic - Holocene |
| Sand | **SB** | Sands and sandstone bedrock | Pliocene - Pleistocene |
| Conglomerate | **CgB** | Gravels and conglomerates bedrock | Pliocene -Pleistocene |
| Clay and Clay flysch | **CFB** | Clay, clayey flysch, phyllites, clayey schists | Cenozoic - Pleistocene |
| Arenaceous flysch | **AFB** | Arenaceous and marly flysch, marly limestones, gypsums, clayey metamorphic rocks | Cenozoic |
| Marly calcareous | **McB** | Marly, calcareous and siliceous successions deposited in pelagic environment | Meso-Cenozoic |
| Calcareous tuff | **CtB** | Calcarenites | Pliocene - Pleistocene |
| Carbonate | **CB** | Limestones, dolostones, marbles | Meso - Cenozoic |
| Igneous metamorphic | **IMB1** | Igneous and metamorphic rocks (Sardegna, Lombardia, Valle d'Aosta, Toscana) | Paleozoic - Cenozoic |
| | **IMB2** | Igneous and metamorphic rocks (Calabria, Sicilia, Liguria) | Meso- Cenozoic |

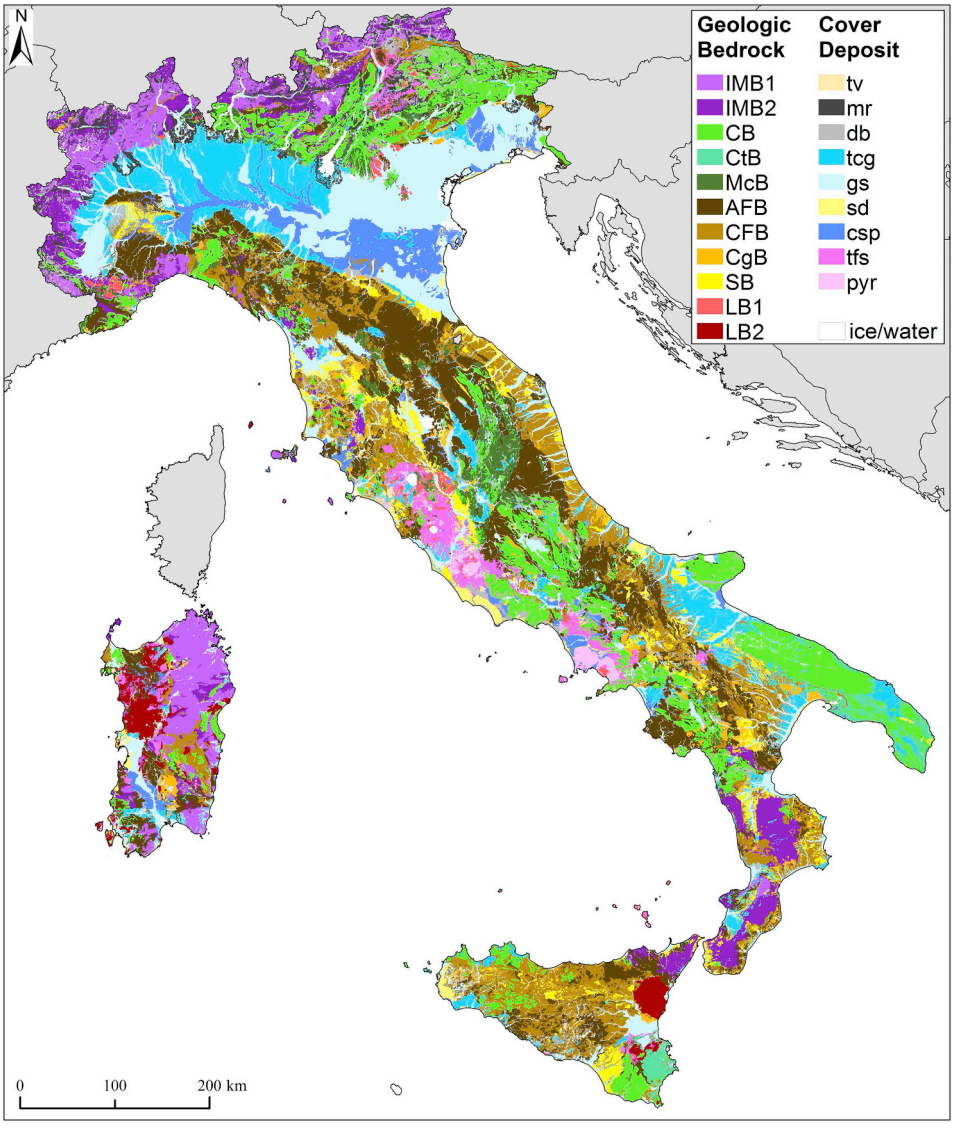


**Fig. 3.** Map of Italy showing the identified geo-lithological complexes (keys in Table 5). Ice or water are reported in white.

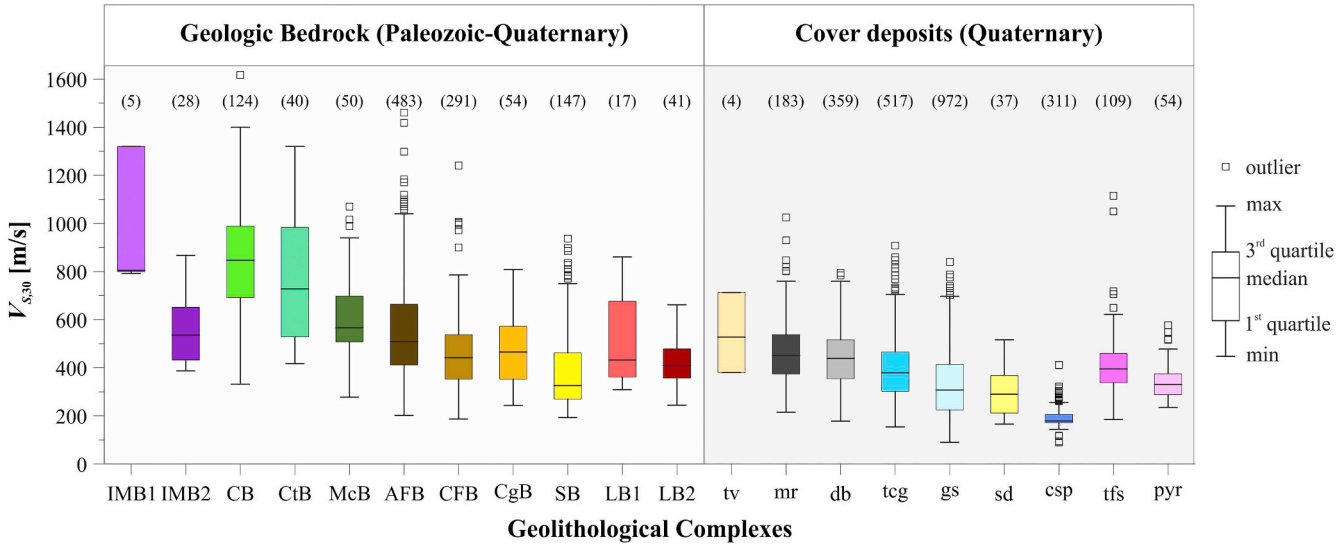


**Fig. 4.** Box-plots showing the distributions of $V_{S,30}$ for the geo-lithological complexes listed in Table 5.

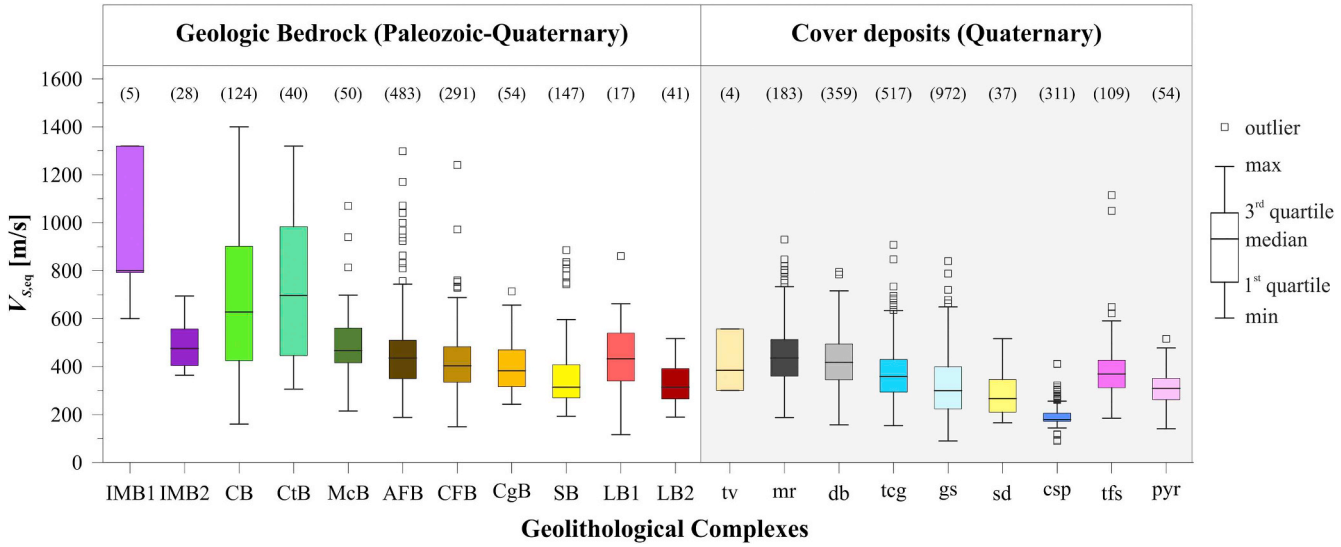


**Fig. 5.** Box-plots showing the distributions of $V_{S,eq}$ values measured by geophysical tests, in the geo-lithological complexes listed in Table 5.

In particular, a value of 20° was considered representative of the critical slope value, above which only thin soils can bury a shallow bedrock, while areas characterized by slope less than 20° can accumulate thicker soils (e.g., Ref. [59]). Following this assumption, LB2 was classified as B and E, the former with slopes higher than 20° and the latter less than 20°. For complex CB, B class is the most frequent, although the analysis of data clearly shows that this complex is characterized by rigid materials, as the sum of A and E classes is greater than class B. These data are also biased by the fact that few investigations are performed on outcrops that are clearly bedrock, hence this complex was also split into sub-areas following the slope proxy, assuming E class where slope is lower than 20°, but assigning A to the slopes higher than 20°.

## 7. Discussion

The code-conforming soil classes are attributed to the polygons of the geo-lithological map as shown in Fig. 9a and Fig. 9b for EC8 and ItBC2018 soil classes, respectively.

Both maps provide, based on a 1:100.000 geologic scale, the seismic soil classifications suitable for large scale studies for which ground motion modifications due to stratigraphic amplification need to be accounted for. At this scale, a reasonable agreement can be observed between both maps, with an enhancement in the ItBC2018 maps, where the area characterized by E class is identified.

The EC8 map highlights a widespread B class distribution (57.4% of the area of Italy), followed by C (19.2%). The soil class A is 18.4% of Italian sites, D is the smallest area (4.2%), E class is not represented. On the ItBC2018 map, B is again the most represented (55.8%), A is lower (13.2%), C and D respectively remain 19.2% and 4.2%, while E class is characterized by 6.8%. In both the EC8 and ItBC2018 maps there are small areas (0.8%) which are not included in any of the soil classes, being representative of ice or water.

In order to discuss the global accuracy of classification, each measured soil class is compared with the inferred soil class of the polygon in which the measurement is enclosed. When the measured class is less stiff than the soil class inferred from the polygon, the site is considered as “overestimated” whereas it is considered as “underestimated” and “matched” when the measured one is stiffer than or equal to the inferred class, respectively (Fig. 10). It can be observed that mismatched values are evenly distributed and local spatially coherent anomalies cannot be identified. Matched sites are the 63% and 60% of the total available measurements for EC8 and ItBC2018, respectively. The overestimation is for 19% and 23% of the sites, whereas an underestimation is for 18% and 17% of the sites with respect to EC8 and

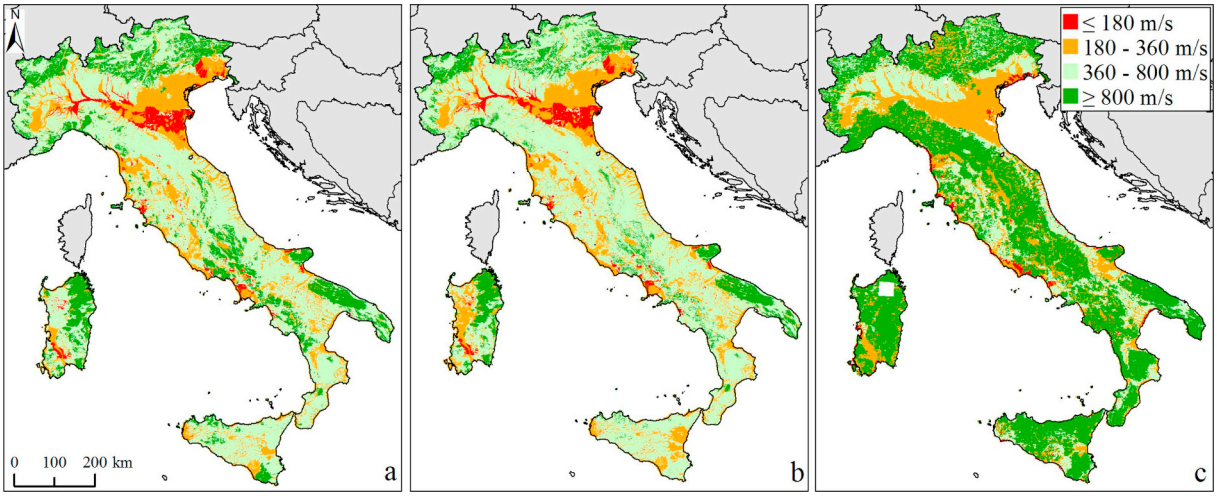


**Fig. 6.** Maps of shear-wave velocity for Italy: (a) and (b) median values of $V_{S,30}$ and $V_{S,eq}$, respectively, according to this study; (c) map of $V_{S,30}$ provided by Ref. [45].

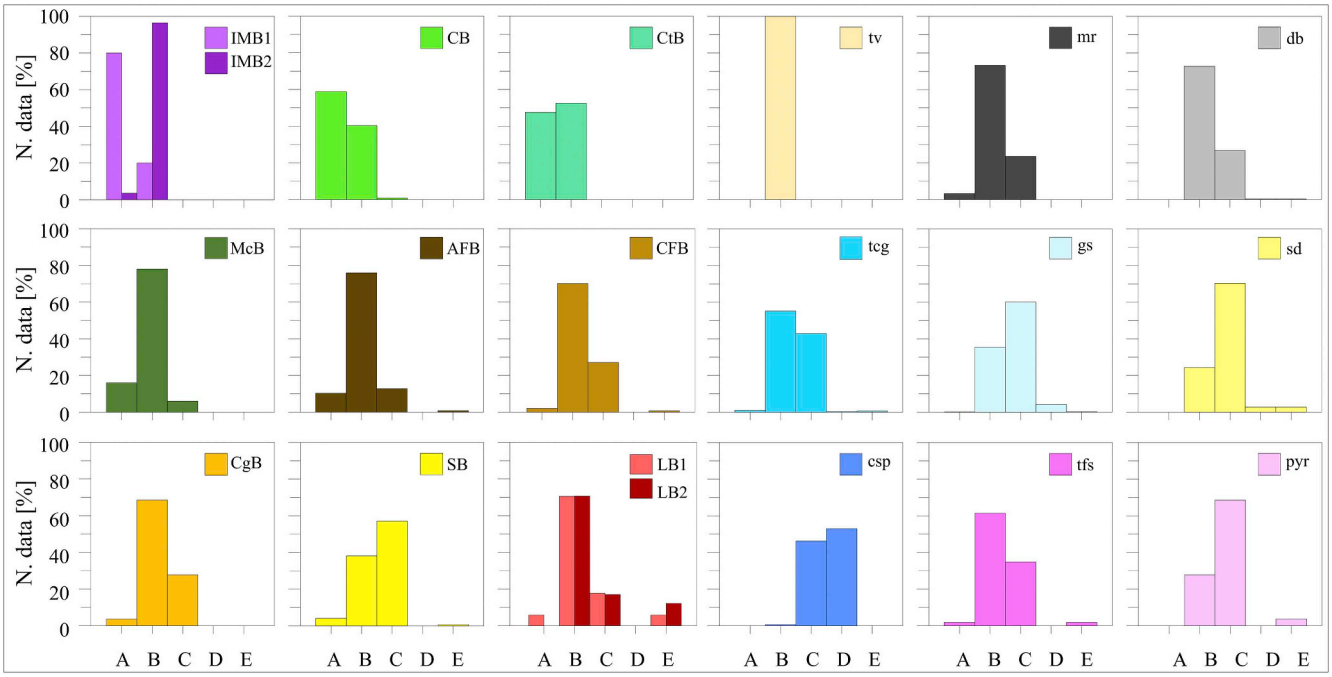


**Fig. 7.** Histograms showing the distributions of soil classes according to EC8 for each geo-lithological complex listed in Table 5.

ItBC2018 classification, respectively.

A more quantitative discussion of EC8 results is provided through Table 6. Each line of the table shows, for each measured soil class, the percentage of sites that are associated to each soil class in the framework of this paper. For example, of the measured soil class A, 39.7% of sites are enclosed into polygons corresponding to site class A in Fig. 9a, 53.2% are enclosed into site class B and 7.1% are in site class C. Thus, 60.3% of the investigated sites from soil class A are underestimated according to the polygons in Fig. 9a. The second line of the table shows that the 71.3% of the total sites classified as soil class B by measurements are equivalently classified by the proposed procedure, while 3.9% and 24.7% are overestimated and underestimated, respectively. Indeed, B and D sites are the best predicted, with 78.6% correctly matched D class. As pertains to C class, half of the cases are correctly predicted (50.0%), while 40.0% are overestimated against 10% of underestimated. Finally, E class is never identified in the proposed procedure and most of investigations sites are attributed to B class (see Fig. 7).

Similarly, Table 7 compares investigations with the soil class map according to ItBC2018. The results are quite similar for B, C, and D classes. E class is also represented; it results correctly matched for 13.8% of cases and it is mainly predicted as B. The A class still results in a poor-quality prediction with only 33.3% of sites correctly matched and 13.1% of cases falling in the E class.

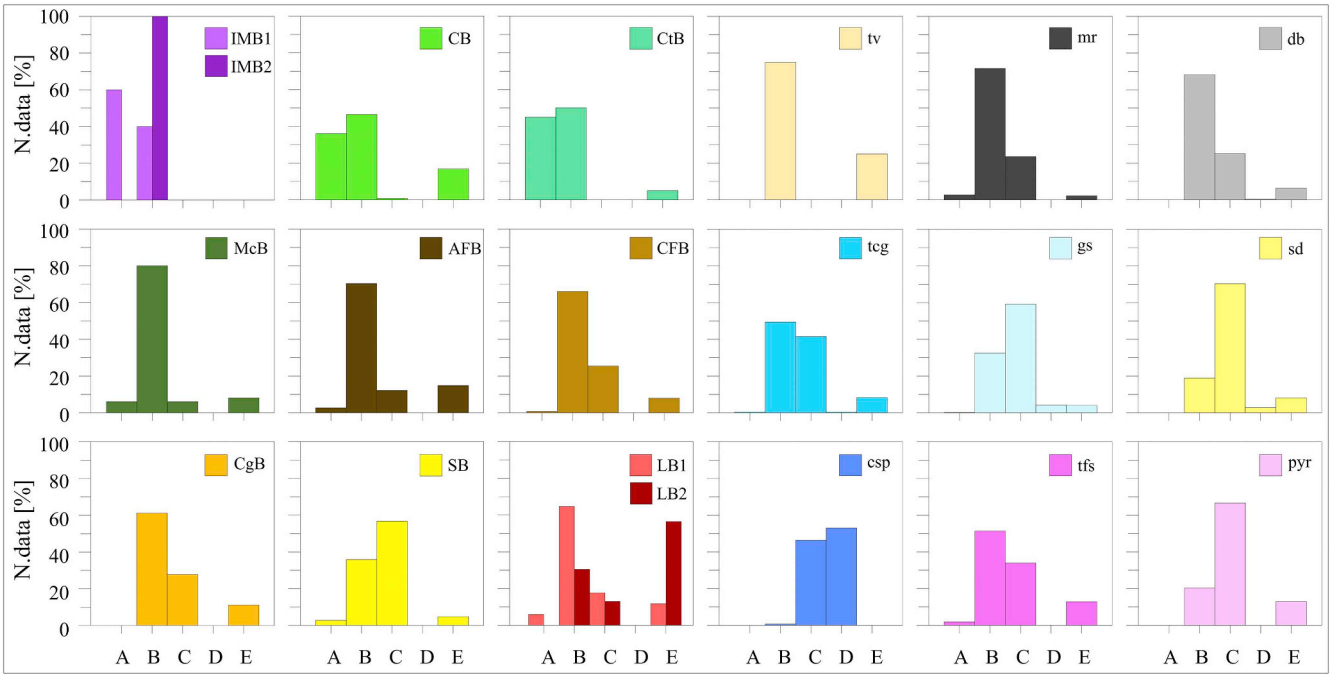


**Fig. 8.** Histograms showing the distributions of soil classes according to ItBC2018 for each geo-lithological complex listed in Table 5.

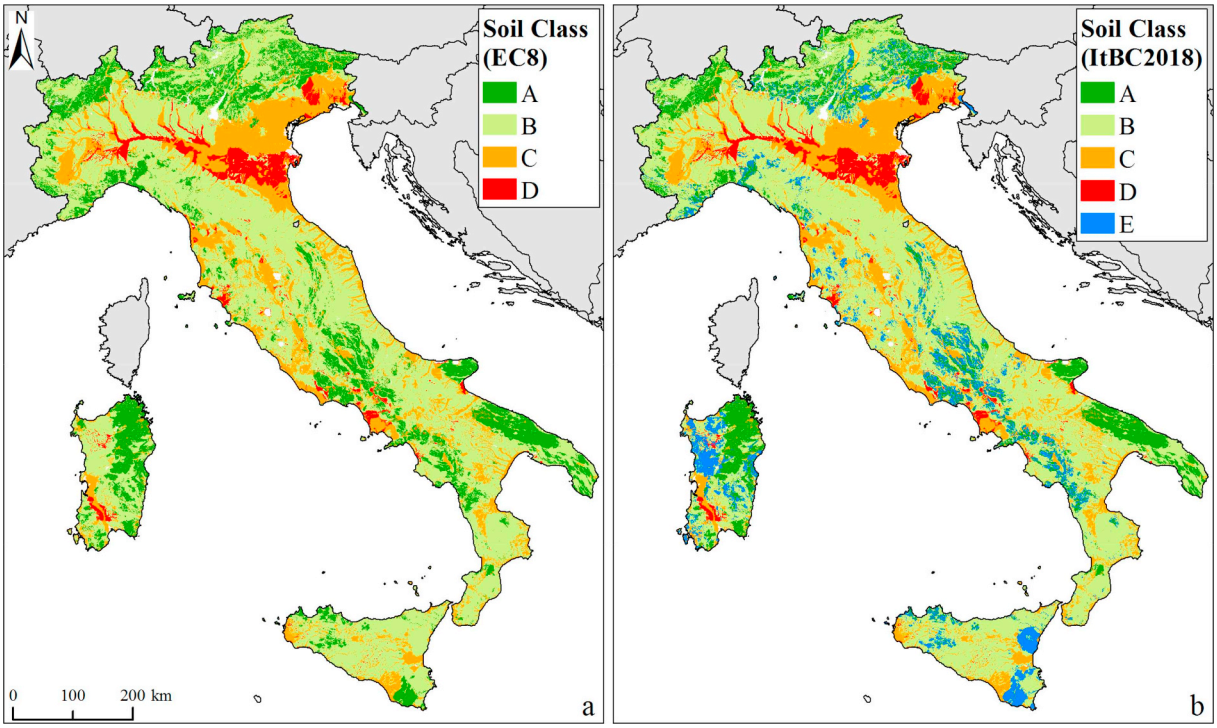


**Fig. 9.** Soil Class maps obtained in accordance with (a) EC8 and (b) ItBC2018. Ice or water are reported in white.

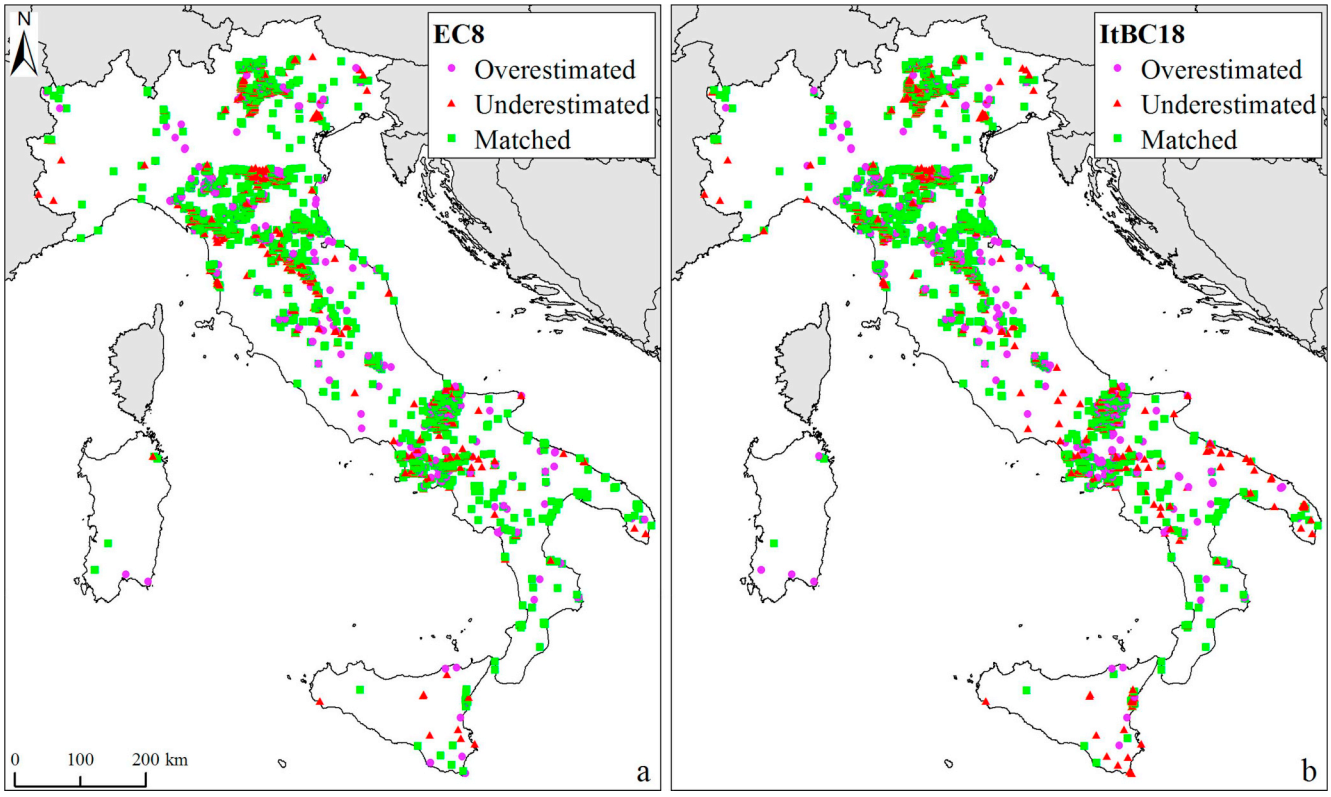


**Fig. 10.** Geographic distribution of comparison between measured and inferred site classes according to (a) EC8 and (b) ItBC2018.

**Table 6**
Comparison between the inferred and the measured classes according to EC8.

| | | Inferred Classes according to EC8 [%] | | | | |
|---|---|---|---|---|---|---|
| | | A | B | C | D | E |
| Measured classes | A | 39.7 | 53.2 | 7.1 | 0.0 | 0.0 |
| | B | 3.9 | 71.3 | 24.7 | 0.1 | 0.0 |
| | C | 0.4 | 39.6 | 50.0 | 10.0 | 0.0 |
| | D | 0.0 | 1.4 | 20.0 | 78.6 | 0.0 |
| | E | 0.0 | 75.0 | 25.0 | 0.0 | 0.0 |

**Table 7**
Comparison between the inferred and the measured classes according to ItBC2018.

| | | Inferred Classes according to ItBC2018 [%] | | | | |
|---|---|---|---|---|---|---|
| | | A | B | C | D | E |
| Measured classes s | A | 33.3 | 46.5 | 7.1 | 0.0 | 13.1 |
| | B | 2.4 | 70.2 | 24.4 | 0.2 | 2.8 |
| | C | 0.3 | 38.4 | 50.6 | 10.1 | 0.6 |
| | D | 0.0 | 1.4 | 20.0 | 78.6 | 0.0 |
| | E | 3.0 | 61.6 | 21.5 | 0.0 | 13.9 |

**Table 8**
Statistics of $V_{S,30}$ measurements for each soil EC8 soil class.

| | $V_{S,30}$ [m/s] | | | |
|---|---|---|---|---|
| | N. of data | Median | Standard deviation | CV |
| A | 129 | 841 | 222 | 0.26 |
| B | 2176 | 444 | 170 | 0.36 |
| C | 1210 | 310 | 133 | 0.39 |
| D | 311 | 179 | 40 | 0.21 |

**Table 9**
Statistics of $V_{S,eq}$ measurements for each soil ItBC2018 soil class.

| | $V_{S,eq}$ [m/s] | | | |
|---|---|---|---|---|
| | N. of data | Median | Standard deviation | CV |
| A | 60 | 831 | 292 | 0.36 |
| B | 2141 | 405 | 145 | 0.34 |
| C | 1214 | 302 | 114 | 0.35 |
| D | 311 | 179 | 40 | 0.21 |
| E | 116 | 403 | 239 | 0.51 |

Finally, results are also discussed in terms of $V_S$ statistics per soil class. To this aim, the measured data are grouped as a function of the EC8 soil class resulting from the discussed procedure (Fig. 9a): the number of observations (N. of data), median, standard deviation and coefficient of variation (CV), that is the ratio of the standard deviation to the mean, of each group of data are reported in Table 8. The table shows a good accordance of median values with the interval identified by EC8 for each soil class (see Table 1). Dispersions of data are not negligible: site class B and C are those with the highest CV and are the classes in which the highest number of observations are located (2176 and 1210, respectively). The lowest number of observations (129) are within site class A and the CV is 0.26 while observations that are comprised in site class D are 311 and the corresponding dispersion of measurements is the lowest, i.e., 0.21; this is because only csp complex is associated to class D.

The equivalent analysis of results is reported in Table 9 referring to $V_{S,eq}$ and the ItBC2018 classification. Median values of measurements located in site classes from A to D are in good accordance with the reference code (see Table 2) whereas measurements pertaining to site class E are higher than what is expected, that is higher than the 100–360 m/s interval. Indeed, as discussed in Section 6, soil class E is identified in the LB2 and CB complexes by introducing the topographic slope as a proxy of the soil characteristics; Table 9 suggested that this strategy can be improved in future development of this work. The CV of B, C and D class are comparable with those of Table 8 while the CV of site class A is higher than the one associated to EC8 soil class.

## 8. Software for data retrieval and illustrative application

To make soil classification available to practitioners, a stand-alone software for database interrogation was developed. It is named Seismic Soil Class-Italy (SSC-Italy) and provides the results of soil classification for any set of sites within the Italian country. The tool is coded in MATHWORKS-Matlab® and benefits from the graphical user interface (GUI) shown in Fig. 11. As first step, the user is required to select the reference code; i.e. EC8 or ItBC2018 (the selected code can be modified at any step of the analysis). In the second step, the user defines the coordinates of the site(s). For each selected site, SSC-Italy provides the corresponding soil class according to the selected code. In addition, various forms of output can be exported: these are the map with the location of the site(s) and a text file with the median(s) and the standard deviation(s) of $V_{S,30}$ (or $V_{S,eq}$) of the polygon(s) containing the site (s), together with the geo-lithological complex(es) the point(s) belongs to.

### 8.1. Rock vs soil probabilistic seismic hazard in Italy

In this section, the importance of soil classification in regional analyses is highlighted via a large-scale application. To this aim, the peak ground acceleration (PGA) resulting from probabilistic seismic hazard analysis (PSHA, e.g. Ref. [60]) on a national scale and characterized by an exceedance return period equal to 475 years, is computed accounting for the polygons of EC8 soil classes derived in this paper. PSHA is performed adopting the same models as the official seismic hazard map used for design (which is provided for rock site conditions only), as described in Ref. [54]. The latter features a logic tree made of several branches and, among them, the branch named 921, in which the Ambraseys et al. [61] GMPE is considered. This branch produces the results that are considered to be the closest to those provided by the full logic tree. The seismic source model is the one of [62] which features 36 seismic source zones. For each zone, the annual rates of earthquakes belonging to discrete bins of magnitude, that is *activity rates*, are adopted (see Ref. [63] for further details). A grid of about ten-thousand points covering the whole territory has been created and, at each site of the grid, the soil class from SSC-Italy is associated. Calculations are carried out with the REASSESS software [64]. Each site is classified in four classes of seismicity as a function of the resulting PGA values, between 0 and 0.1 g, 0.1 g and 0.2 g, 0.2 g and 0.3 g, 0.3 g and 0.4 g.

The described analysis is then repeated assuming rock conditions for all the sites in order to compare the resulting seismicity classes. The maps for comparison are given in Fig. 12 together with the seismic sources of [62]. For rock site conditions (Fig. 12a), the first class includes the 33.2% of the sites, while 48.7% and 18.1% of the sites are obtained for the second and third hazard classes, respectively. Since the maximum PGA value on rock across Italy is equal to 0.27 g, no sites can be found in the fourth seismicity class. Due to the soil effects and considering the same exceedance return period (Fig. 12b), the percentage of sites within the first and second class reduces to 23.2% and 37.4%, respectively. The sites with PGA in the range between 0.2 g and 0.3 g cover the 31.8% of the territory and, in the remaining 7.6% of sites, accelerations are between 0.3 g and 0.4 g.

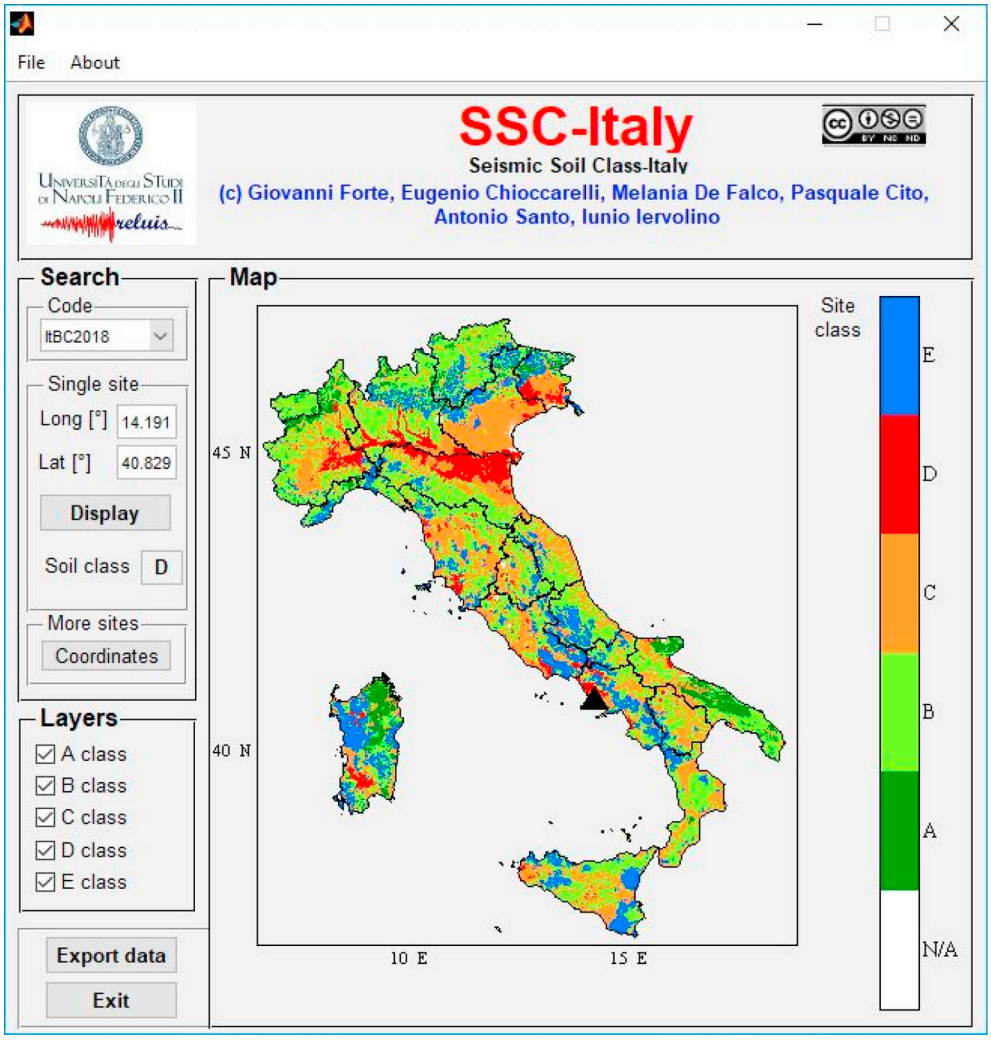


**Fig. 11.** Main GUI of SSC-Italy software.

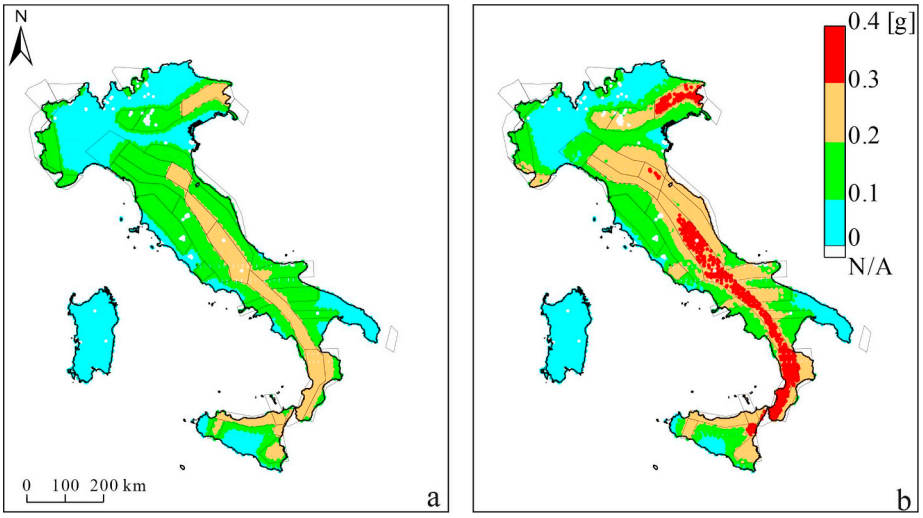


**Fig. 12.** Seismic classification for Italy on (a) rock and (b) soil site condition; the sites in which the PGA is not assigned (N/A) are those belonging to the ice/water category of Fig. 3.

## 9. Conclusions

The study discussed in this paper addresses the issue of soil classification in Italy, which may be required, for example, for large scale seismic risk analyses or post-earthquake shakemap generation. In these cases, although site-specific seismic propagation analyses are not feasible, an approximate characterization of soil dynamic behaviour is required. The latter, which may be represented by the knowledge of $V_{S,30}$ or $V_{S,eq}$ is usually not available. On the other hand, large-scale geological maps are often available, but they do not include appropriate information for soil characterization in seismic conditions.

In the study, a four-step procedure to correlate the surface geological maps with site-specific investigations was presented and discussed. It was implemented for Italy, where geological maps at 1:100.000 scale are available, together with a large database of site specific investigations that were collected. The results, which can be upgraded as new site specific investigations become available, are maps of soil characteristics in terms of median and standard deviation $V_{S,30}$ and $V_{S,eq}$ values as well as soil classification according to EC8 and ItBC2018. They have been rendered publicly accessible through a simple stand-alone software (SSC-Italy) available at http://wpage.unina.it/iuniervo/SSC-Italy.zip.

The soil classes measured via site-specific investigations have been compared to the soil classes inferred from the maps. For EC8, in the 63% of sites the soil class is correctly matched whereas in 18% and 19% of cases soil classes are underestimated and overestimated, respectively. Similar percentages are obtained for ItBC2018 classification: 60% of sites are correctly matched, 17% are underestimated and 23% are overestimated.

To assess the effect of soil classification on a national scale, an illustrative application has been developed. It is the seismic hazard map of Italy in terms of PGA with 475-years return period on soil compared to the corresponding seismic hazard map computed for rock. Due to models adopted for computation, the latter is a good approximation of the national official seismic hazard.

It is important to finally remark that the derived results are not appropriate at all for site-specific studies as they do not replace microzonation and local site response studies, which require more detailed investigations for the soil site characterization and the structural design.

## Acknowledgements

The authors acknowledge dr. Giovanni Lanzano and the other anonymous reviewers, whose comments and suggestions improved the overall manuscript. Grateful acknowledgments are due to dr. Giuseppe Di Crescenzo for the fruitful scientific contribution provided in the early stage of this research. Moreover, dr. Georgios Baltzopoulos is gratefully acknowledged for proofreading the manuscript.

## Appendix

Figs. 4 and 5 summarize data distribution for each geo-lithological complex. The numerical value of mean, median and standard deviation of data for each complex are reported in the following table in term of $V_{S,30}$ and $V_{S,eq}$.

Table A

| Acronym | $V_{S,30}$ [m/s] | | | $V_{S,eq}$ [m/s] | | |
|---|---|---|---|---|---|---|
| | Mean | Median | Standard deviation | Mean | Median | Standard deviation |
| IMB1 | 981 | 805 | 254 | 863 | 800 | 269 |
| IMB2 | 556 | 536 | 132 | 490 | 476 | 92 |
| CB | 855 | 847 | 221 | 670 | 628 | 302 |
| CtB | 777 | 728 | 253 | 741 | 697 | 287 |
| McB | 612 | 566 | 178 | 494 | 467 | 156 |
| AFB | 550 | 509 | 195 | 451 | 436 | 155 |
| CFB | 458 | 442 | 150 | 416 | 403 | 124 |
| CgB | 474 | 466 | 148 | 401 | 383 | 100 |
| SB | 384 | 326 | 168 | 355 | 315 | 133 |
| LB1 | 511 | 432 | 172 | 439 | 432 | 177 |
| LB2 | 419 | 409 | 84 | 329 | 315 | 80 |
| tv | 537 | 528 | 138 | 407 | 384 | 108 |
| mr | 465 | 451 | 141 | 455 | 436 | 138 |
| db | 441 | 439 | 120 | 424 | 418 | 117 |
| tcg | 396 | 379 | 132 | 367 | 360 | 108 |
| gs | 333 | 308 | 129 | 320 | 300 | 112 |
| sd | 296 | 290 | 96 | 284 | 267 | 89 |
| csp | 195 | 179 | 40 | 195 | 179 | 40 |
| tfs | 418 | 395 | 138 | 385 | 369 | 131 |
| pyr | 346 | 331 | 83 | 317 | 309 | 77 |

*Data sources*

In addition to the cited references, data used in this study were readily accessible from the following sources (last accessed 18/09/2018):

- Italian accelerometric archive ITACA (http://itaca.mi.ingv.it);
- Seismic microzonation of Abruzzo Region (https://protezionecivile.regione.abruzzo.it/index.php/microzonazione);
- Seismic microzonation of Basilicata Region (http://www.crisbasilicata.it/microzonazione/index.html);
- Regional Seismological and Geological Service of Emilia Romagna Region (http://geo.regione.emilia-romagna.it/geocatalogo/);
- Regional Seismological and Geological Service of Molise Region (http://www3.regione.molise.it/flex/cm/pages/ServeBLOB.php/L/IT/IDPagina/381);
- Civil Protection of Catania for Sicilia Region (http://sit.protezionecivilesicilia.it/opcm3278/);
- VEL project for Toscana Region (http://www.regione.toscana.it/-/banca-dati-vel);

- Civil Protection of Trento for Trentino Alto-Adige (http://www.protezionecivile.tn.it/);
- Regional Seismological and Geological Service of Umbria Region (http://storicizzati.territorio.regione.umbria.it/Static/IndaginiGeologicheKmz/Index_kmz.htm);

## Funding

This research was funded by the Italian Civil Protection Department RELUIS project 2010–2013, RS2 Task 2.1, 2.2 “Definition of geological models and site amplification for impulsive earthquakes near-source". The opinions and conclusions presented by the authors do not necessarily reflect those of the funding entity.

## References

[1] Kramer SL. Geotechnical earthquake engineering. Upper Saddle River, New Jersey: Prentice-Hall, Inc.; 1996. 07458.
[2] Dobry R, Vucetic M. International symposium of geotechnical engineering of soft soils. Dyn. Prop. Seism. response soft clay Depos. 1987:51–87.
[3] Seed RB, Dickenson SE, Idriss IM. Principal geotechnical aspects of the 1989 Loma Prieta earthquake. Soils Found 1991;31:1–26. https://doi.org/10.3208/sandf1972.31.1.
[4] Gautam D, Forte G, Rodrigues H. Site effects and associated structural damage analysis in Kathmandu Valley, Nepal. Earthquakes Struct 2016;10:1013–32. https://doi.org/10.12989/eas.2016.10.5.1013.
[5] Jeong S, Bradley BA. Amplification of strong ground motions at Heathcote Valley during the 2010–2011 Canterbury earthquakes: observation and 1D site response analysis. Soil Dynam Earthq Eng 2017;100:345–56. https://doi.org/10.1016/J.SOILDYN.2017.06.004.
[6] Sextos A, De Risi R, Pagliaroli A, Foti S, Passeri F, Ausilio E, et al. Local site effects and incremental damage of buildings during the 2016 Central Italy earthquake sequence. Earthq Spectra 2018. https://doi.org/10.1193/100317EQS194M. 100317EQS194M.
[7] Bradley BA. A framework for validation of seismic response analyses using seismometer array recordings. Soil Dynam Earthq Eng 2011;31:512–20. https://doi.org/10.1016/J.SOILDYN.2010.11.008.
[8] Elgamal A-W, Zeghal M, Parra E, Gunturi R, Tang HT, Stepp JC. Identification and modeling of earthquake ground response — I. Site amplification. Soil Dynam Earthq Eng 1996;15:499–522. https://doi.org/10.1016/S0267-7261(96)00021-8.
[9] Borcherdt RD, Glassmoyer G. On the characteristics of local geology and their influence on ground motions generated by the Loma Prieta earthquake in the San Francisco Bay region, California. Bull Seismol Soc Am 1992;82:603–41.
[10] Borcherdt RD. Estimates of site-dependent response spectra for design (methodology and justification). Earthq Spectra 1994;10:617–53. https://doi.org/10.1193/1.1585791.
[11] Comina C, Foti S, Boiero D, Socco LV. Reliability of VS,30 evaluation from surface-wave tests. J Geotech Geoenviron Eng 2011;137:579–86. https://doi.org/10.1061/(ASCE)GT.1943-5606.0000452.
[12] Ohta Y, Goto N. Empirical shear-wave velocity equations in terms of characteristic soil indexes. Earthq Eng Struct Dyn 1978;6:167–87. https://doi.org/10.1002/eqe.4290060205.
[13] Pitilakis K, Raptakis D, Lontzetidis K, Tika-Vassilikou T, Jongmans D. Geotechnical and geophysical description of euro-seistests, using field and laboratory tests and moderate strong ground motions. J Earthq Eng 1999;3:381–409. https://doi.org/10.1080/13632469909350352.
[14] Fabbrocino S, Lanzano G, Forte G, Santucci de Magistris F, Fabbrocino G. SPT blow count vs. shear-wave velocity relationship in the structurally complex formations of the Molise Region (Italy). Eng Geol 2015;187:84–97. https://doi.org/10.1016/J.ENGGEO.2014.12.016.
[15] Boore DM, Stewart JP, Seyhan E, Atkinson GM. NGA-West2 equations for predicting PGA, PGV, and 5% damped PSA for shallow crustal earthquakes. Earthq Spectra 2014;30:1057–85. https://doi.org/10.1193/070113EQS184M.
[16] Campbell KW, Bozorgnia Y. NGA-West2 ground motion model for the average horizontal components of PGA, PGV, and 5% damped linear acceleration response spectra. Earthq Spectra 2014;30:1087–115. https://doi.org/10.1193/062913EQS175M.
[17] Akkar S, Sandıkkaya MA, Bommer JJ. Empirical ground-motion models for point- and extended-source crustal earthquake scenarios in Europe and the Middle East. Bull Earthq Eng 2014;12:359–87. https://doi.org/10.1007/s10518-013-9461-4.
[18] Lanzano G, Luzi L, Pacor F, Felicetta C, Puglia R, Sgobba S, et al. A revised ground-motion prediction model for shallow crustal earthquakes in Italy n.d. doi:10.1785/0120180210.
[19] Akkar S, Bommer JJ. Empirical equations for the prediction of PGA, PGV, and spectral accelerations in Europe, the Mediterranean Region, and the Middle East. Seismol Res Lett 2010;81:195–206. https://doi.org/10.1785/gssrl.81.2.195.
[20] Bindi D, Pacor F, Luzi L, Puglia R, Massa M, Ameri G, et al. Ground motion prediction equations derived from the Italian strong motion database. Bull Earthq Eng 2011;9:1899–920. https://doi.org/10.1007/s10518-011-9313-z.
[21] Bindi D, Massa M, Luzi L, Ameri G, Pacor F, Puglia R, et al. Pan-European ground-motion prediction equations for the average horizontal component of PGA, PGV, and 5 %-damped PSA at spectral periods up to 3.0 s using the RESORCE dataset. Bull Earthq Eng 2014;12:391–430. https://doi.org/10.1007/s10518-013-9525-5.
[22] Cauzzi C, Faccioli E. Broadband (0.05 to 20 s) prediction of displacement response spectra based on worldwide digital records. J Seismol 2008;12:453–75. https://doi.org/10.1007/s10950-008-9098-y.
[23] BSSC. NEHRP Recommended provisions for seismic regulations for new buildings and other structures. 1998.
[24] CEN. European Committee for Standardization. Eurocode 8: design provisions for earthquake resistance of structures 2003.
[25] Steidl JH. Site response in Southern California for probabilistic seismic hazard analysis. Bull Seismol Soc Am 2000;90:S149–69. https://doi.org/10.1785/0120000504.
[26] Choi Y, Stewart JP. Nonlinear site amplification as function of 30 m shear-wave velocity. Earthq Spectra 2005;21:1–30. https://doi.org/10.1193/1.1856535.
[27] Lee VW, Trifunac MD. Should average shear-wave velocity in the top 30 m of soil be used to describe seismic amplification? Soil Dynam Earthq Eng 2010;30:1250–8. https://doi.org/10.1016/J.SOILDYN.2010.05.007.
[28] Anbazhagan P, Sheikh MN, Parihar A. Influence of rock depth on seismic site classification for shallow bedrock regions. Nat Hazards Rev 2013;14:108–21. https://doi.org/10.1061/(ASCE)NH.1527-6996.0000088.
[29] Bouckovalas G, Papadimitriou A, Karamitros D. Compatibility of EC-8 ground types and site effects with 1-D wave propagation theory. Proceedings of ETC-12 Workshop, Jan 20-21, Athens. 1992.
[30] Pitilakis K, Riga E, Anastasiadis A. New code site classification, amplification factors and normalized response spectra based on a worldwide ground-motion database. Bull Earthq Eng 2013;11:925–66. https://doi.org/10.1007/s10518-013-9429-4.
[31] CS.LL.PP. Decreto Ministeriale: norme tecniche per le costruzioni, Gazzetta Ufficiale della Repubblica Italiana, n. 42, 20 febbraio, Suppl. Ordinario n. 8. Ist. Polig. Rome: e Zecca dello Stato S.p.a.; 2018. (in Italian).
[32] ISSMGE. Manual for zonation on seismic geotechnical hazards (revised version). 1993.
[33] Ansal A, Kurtuluş A, Tönük G. Seismic microzonation and earthquake damage scenarios for urban areas. Soil Dynam Earthq Eng 2010;30:1319–28. https://doi.org/10.1016/J.SOILDYN.2010.06.004.
[34] Wills CJ, Clahan KB. Developing a map of geologically defined site-condition categories for California. Bull Seismol Soc Am 2006;96:1483–501. https://doi.org/10.1785/0120050179.
[35] Chiou B, Darragh R, Gregor N, Silva W. NGA project strong-motion database. Earthq Spectra 2008;24:23–44. https://doi.org/10.1193/1.2894831.
[36] Lee C-T, Tsai B-R. Mapping Vs30 in Taiwan. Terr Atmos Ocean Sci 2008;19:671. https://doi.org/10.3319/TAO.2008.19.6.671(PT).
[37] Cantore L, Convertito V, Zollo A. Development of a site-conditions map for the Campania-Lucania region (southern Apennines, Italy). Ann Geophys 2010;53:27–37. https://doi.org/10.4401/ag-4648.
[38] Yong A. Comparison of measured and proxy-based V S 30 values in California. Earthq Spectra 2016;32:171–92. https://doi.org/10.1193/013114EQS025M.
[39] Parker GA, Harmon JA, Stewart JP, Hashash YMA, Kottke AR, Rathje EM, et al. Proxy-based $V_{S30}$ estimation in central and eastern North America. Bull Seismol Soc Am 2017;107:117–31. https://doi.org/10.1785/0120160101.
[40] Thompson EM, Wald DJ, Worden CB. A VS30 map for California with geologic and topographic constraints. Bull Seismol Soc Am 2014;104:2313–21. https://doi.org/10.1785/0120130312.
[41] Allen TI, Wald DJ. Topographic slope as a proxy for seismic site-conditions (VS30) and amplification around the globe. 2007. https://doi.org/10.3133/OFR20071357.
[42] Lemoine A, Douglas J, Cotton F. Testing the applicability of correlations between topographic slope and VS30 for Europe. Bull Seismol Soc Am 2012;102:2585–99. https://doi.org/10.1785/0120110240.
[43] Forte G, Fabbrocino S, Fabbrocino G, Lanzano G, Santucci de Magistris F, Silvestri F. A geolithological approach to seismic site classification: an application to the Molise Region (Italy). Bull Earthq Eng 2017;15:175–98. https://doi.org/10.1007/s10518-016-9960-1.
[44] Luzi L, Meroni F. Deliverable 6: valutazioni sperimentali di amax e di spettri di risposta calibrate per le condizioni locali. 2007. (in italian).
[45] Michelini A, Faenza L, Lauciani V, Malagnini L. Shakemap implementation in Italy. Seismol Res Lett 2008;79:688–97. https://doi.org/10.1785/gssrl.79.5.688.
[46] Di Capua G, Peppoloni S, Amanti M, Cipolloni C, Conte G. Site classification map of Italy based on surface geology. Geol Soc London, Eng Geol Spec Publ 2016;27:147–58. https://doi.org/10.1144/EGSP27.13.
[47] Wald DJ, Quitoriano V, Heaton TH, Kanamori H, Scrivner CW, Worden CB. TriNet “ShakeMaps”: rapid generation of peak ground motion and intensity maps for earthquakes in Southern California. Earthq Spectra 1999;15:537–55. https://doi.org/10.1193/1.1586057.
[48] Pal JD, Atkinson GM. Scenario shakemaps for Ottawa, Canada. Bull Seismol Soc Am 2012;102:650–60. https://doi.org/10.1785/0120100302.
[49] CS.LL.PP. Decreto Ministeriale 14 gennaio 2008: norme tecniche per le costruzioni, Gazzetta Ufficiale della Repubblica Italiana, n. 29, 4 febbraio, Suppl. Ordinario n. 30. Ist. Polig. e Zecca dello Stato S.p.a., Rome. 2008. (in Italian).
[50] Boore DM. Estimating Vs (30) (or NEHRP site classes) from shallow velocity models (depths < 30 m) vol. 94. 2004.
[51] Boore DM, Thompson EM, Cadet H. Regional correlations of VS30 and velocities averaged over depths less than and greater than 30 meters. Bull Seismol Soc Am 2011;101:3046–59. https://doi.org/10.1785/0120110071.

[52] Kuo C-H, Wen K-L, Hsieh H-H, Chang T-M, Lin C-M, Chen C-T. Evaluating empirical regression equations for Vs and estimating Vs30 in northeastern Taiwan. Soil Dynam Earthq Eng 2011;31:431–9. https://doi.org/10.1016/J.SOILDYN.2010.09.012.
[53] ASTM. D7400-19 Standard test methods for downhole seismic testing. PA: ASTM International; 2019https://doi.org/10.1520/D7400_D7400M-19.
[54] Stucchi M, Meletti C, Montaldo V, Crowley H, Calvi GM, Boschi E. Seismic hazard assessment (2003-2009) for the Italian building code. Bull Seismol Soc Am 2011;101:1885–911. https://doi.org/10.1785/0120100130.
[55] Amanti M, Bontempo R, Cara P, Conte G, Di Bucci D, Lembo P, et al. Interactive geological map of Italy, 1:100.000. SGN, SSN, ANAS 3 CD-Rom. 2002.
[56] Stewart JP, Klimis N, Savvaidis A, Theodoulidis N, Zargli E, Athanasopoulos G, et al. Compilation of a local VS profile database and its application for inference of VS30 from geologic- and terrain-based proxies. Bull Seismol Soc Am 2014;104:2827–41. https://doi.org/10.1785/0120130331.
[57] Peccerillo A. Plio-Quaternary volcanism in Italy : petrology, geochemistry, geodynamics. Springer; 2005.
[58] Hubert M, Vandervieren E, Larsen WA. An adjusted boxplot for skewed distributions. Comput Stat Data Anal 2008;52(12):5186–201https://doi.org/10.1016/j.csda.2007.11.008.
[59] Horton RE. Erosional development of streams and their and their drainage basins; hydrophysical approach to quantitative morphology. GSA Bull 1945;56:275–370. https://doi.org/10.1130/0016-7606(1945)56[275:edosat]2.0.co;2.
[60] Cornell CA. Engineering seismic risk analysis. Bull Seismol Soc Am 1968;58:1583–606https://doi.org/10.1016/0167-6105(83)90143-5.
[61] Ambraseys NN, Simpson KA, Bommer JJ. Prediction of horizontal response spectra in Europe. Earthq Eng Struct Dyn 1996;25:371–400. https://doi.org/10.1002/(SICI)1096-9845(199604)25:4<371::AID-EQE550>3.0.CO;2-A.
[62] Meletti C, Galadini F, Valensise G, Stucchi M, Basili R, Barba S, et al. A seismic source zone model for the seismic hazard assessment of the Italian territory. Tectonophysics 2008;450:85–108. https://doi.org/10.1016/j.tecto.2008.01.003.
[63] Iervolino I, Chioccarelli E, Giorgio M. Aftershocks' effect on structural design actions in Italy. Bull Seismol Soc Am 2018;108:2209–20. https://doi.org/10.1785/0120170339.
[64] Chioccarelli E, Cito P, Iervolino I, Giorgio M. REASSESS V2.0: software for single- and multi-site probabilistic seismic hazard analysis. Bull Earthq Eng 2018:1–25. https://doi.org/10.1007/s10518-018-00531-x.